International Journal of Food Microbiology 306 (2019) 108265

Contents lists available at ScienceDirect

International Journal of Food Microbiology

journal homepage: www.elsevier.com/locate/ijfoodmicro

A proteomic investigation of *Aspergillus carbonarius* exposed to yeast volatilome or to its major component 2-phenylethanol reveals major shifts in fungal metabolism

Bruno Tilocca[a], Virgilio Balmas[a,c], Zahoor Ul Hassan[b], Samir Jaoua[b], Quirico Migheli[a,c,*]

[a] Dipartimento di Agraria, Università degli Studi di Sassari, Viale Italia 39, I-07100 Sassari, Italy
[b] Department of Biological & Environmental Sciences, College of Arts and Sciences, Qatar University, P.O. Box: 2713, Doha, Qatar
[c] Unità di Ricerca Istituto Nazionale di Biostrutture e Biosistemi, Università degli Studi di Sassari, Viale Italia 39, I-07100 Sassari, Italy

ARTICLE INFO

Keywords:
Biological control
Volatile organic compounds
Ochratoxin A
Mycotoxigenic fungi
Mycotoxins
Biosynthetic routes

ABSTRACT

The use of yeast-derived volatile organic compounds (VOCs) represents a promising strategy for the biological control of various plant pathogens, including mycotoxin-producing fungi. Previous studies demonstrated the efficacy of the low-fermenting yeast *Candida intermedia* isolate 253 in reducing growth, sporulation, and ochratoxin A biosynthesis by *Aspergillus carbonarius* MPVA566. This study aimed to investigate whether the inhibitory effect of the yeast volatilome is solely attributable to 2-phenylethanol, its major component, or if a synergistic effect of all volatilome components is required to achieve an effective control of the fungal growth and metabolism. Microbiological methods, HPLC measurements and a UPLC-MS/MS approach were used to investigate the metabolic profile of *A. carbonarius* MPVA566 at different growing conditions: standard incubation (control), exposed to *C. intermedia* 253 volatilome, and incubation in the presence of 2-phenylethanol. Both yeast volatilome and 2-phenylethanol succeeded in the macroscopic inhibition of the radial mycelial growth, along with a significant reduction of ochratoxin A production. Functional classification of the fungal proteome identified in the diverse growing conditions revealed a different impact of both yeast VOCs and 2-phenylethanol exposure on the fungal proteome. Yeast VOCs target an array of metabolic routes of fungal system biology, including a marked reduction in protein biosynthesis, proliferative activity, mitochondrial metabolism, and particularly in detoxification of toxic substances. Exposure to 2-phenylethanol only partially mimicked the metabolic effects observed by the whole yeast volatilome, with protein biosynthesis and proliferative activity being reduced when compared with the control samples, but still far from the VOCs-exposed condition. This study represents the first investigation on the effects of yeast-derived volatilome and 2-phenylethanol on the metabolism of a mycotoxigenic fungus by means of proteomics analysis.

Chemical compounds studied or used in this article: 2-Phenylethanol (PubChem CID: 6054); ochratoxin-A (PubChem CID: 442530); sodium dodecyl sulfate (PubChem CID: 3423265); dithiothreitol (PubChem CID: 446094); phenylmethylsulfonyl fluoride (PubChem CID: 4784); iodoacetamide (PubChem CID: 3727); ammonium bicarbonate (PubChem CID: 14013); acetic acid (PubChem CID: 176); and acetonitrile (PubChem CID: 6342).

1. Introduction

Pre- and post-harvest loss of fruit and other agricultural commodities due to filamentous fungi contamination occurs frequently in both industrialised and developing countries (Nunes, 2012). Besides representing a significant economic loss, the contamination of agricultural commodities by mycotoxigenic fungi is also an important threat to human and animal health (Liu et al., 2013; Nunes, 2012). Major mycotoxin-producing fungi include different species belonging to the genera *Fusarium*, *Aspergillus* and *Penicillium*, with *Aspergillus carbonarius* being one of the most relevant producers of ochratoxin A (OTA) in food and feedstuff (Kogkaki et al., 2015).

The kidney is the principal target of OTA (Bui-Klimke and Wu, 2015), where this mycotoxin exerts a renal carcinogenic effect. Moreover, its toxicity is linked to immunotoxicity, inhibition of both protein biosynthesis and mitochondrial respiration, and increased lipid

* Corresponding author at: Dipartimento di Agraria, Università degli Studi di Sassari, Viale Italia 39, I-07100 Sassari, Italy.
E-mail address: qmigheli@uniss.it (Q. Migheli).

https://doi.org/10.1016/j.ijfoodmicro.2019.108265
Received 9 May 2019; Received in revised form 2 July 2019; Accepted 9 July 2019
Available online 10 July 2019

peroxidation (Bondy and Pestka, 2000; Duarte et al., 2011). The International Agency for Research on Cancer (IARC) has classified OTA as a Group 2B possible human carcinogen, on the basis of previous animal tests (Fazekas et al., 2005; Haighton et al., 2012). Owing to the wide array of adverse effects, the European Union imposed strict regulations, setting the maximum limit of OTA at 2 ppb in wine and other grape-derived products and at 5 ppb in all cereal grains for human consumption (Commission Regulation (EC) No. 1881/2006).

Preventing OTA contamination in food and feed commodities at both pre- and post-harvest stages would benefit human health, crop yield and marketability of the agricultural (and derived) products.

To date, fungicides are the major routes employed to control plant pathogens. However, long-term exposure to synthetic fungicides has frequently generated the selection of resistant mutants among plant pathogenic fungi. Fungicide resistance is considered one of the biggest issues in modern agriculture, since it impacts not only the agricultural field: several cases of cross-resistance to fungicides (*e.g.* azoles), widely adopted in both clinical and agricultural environment, were observed in recent years. Known examples of azole resistance include *Aspergillus fumigatus* (Snelders et al., 2008), *Candida albicans* (Pfaller and Diekema, 2004) and *Cryptococcus neoformans* (Deising et al., 2008; Lucas et al., 2015). Due to the increasing incidence of fungicide resistance mechanisms, along with the harmful effects of pesticide residues on human health and on the environment, it is realistic to expect major restrictions on the use of synthetic fungicides in agriculture in the near future (Adaskaveg and Förster, 2009; Brent and Hollomon, 2007; Tribe et al., 2006). In this scenario, the application of biological control agents (BCAs) represents a valuable alternative to prevent mycotoxin contamination (Liu et al., 2013; Nunes, 2012; Spadaro and Gullino, 2004). Among the diverse biological control strategies, the use of antagonistic yeasts is receiving steadily increasing attention. Yeasts have simple nutritional requirements, they are capable of colonising a variety of surfaces, featured by diverse physicochemical properties, and produce natural antimicrobial compounds that have no harmful effects on humans and animals (Farbo et al., 2018; Fiori et al., 2014; Liu et al., 2011a, 2011b). Also, their usage can be sized to large scale applications and do not produce allergens or other secondary metabolites as other BCAs might do (Melin et al., 2007).

Diverse modes of action of yeasts as BCAs are currently exploited; among these, the production of volatile organic compounds (VOCs) has raised increasing attention (Nunes, 2012). VOCs are low molecular weight metabolites featured by a low vapour pressure, and have shown effectiveness in the inhibition of the growth and sporulation of a wide range of fungi, as well as by reducing the expression of genes putatively involved in mycotoxin biosynthesis (Chang et al., 2015; Melin et al., 2007).

Previous studies demonstrated the inhibitory effect of four low- or non-fermenting yeast strains against the OTA-producing fungus *A. carbonarius* (Fiori et al., 2014). These findings were successively confirmed in a companion study where a GC–MS investigation of the yeasts volatilome identified 2-phenylethanol (2-PE) as the major component of the molecular cocktail featuring the VOCs composition of all tested antagonistic yeast strains (Farbo et al., 2018).

The main objective of this study was to investigate whether the administration of the sole 2-PE reflects the metabolic effect attributed to the yeast VOCs administration. We adopted a proteomic approach to investigate the effect of 2-PE on the metabolic asset of *A. carbonarius*. The resulting proteomic profile was comparatively evaluated against the protein repertoire expressed by this fungus grown under standard conditions, or in the presence of *Candida intermedia* 253, a low-fermenting yeast strain already selected in the previous studies for its remarkable antagonistic features. Details on the metabolic impact of each treatment on the fungal metabolic asset are provided.

2. Materials and methods

2.1. Fungal and yeast cultures

A. carbonarius Bainier Thom. MPVA566 (courtesy of Professor Paola Battilani, Università Cattolica del Sacro Cuore, Piacenza, Italy) is maintained in the mycological collection of the Department of Agricultural Sciences, University of Sassari (Italy) and routinely grown on PDA (potato dextrose agar; Sigma-Aldrich, St. Louis, MO, USA) at 25 °C for 7 days (Farbo et al., 2018).

C. intermedia 253 strain was grown on YPD agar (1% yeast extract, 2% peptone, 2% dextrose, 2% agar; Sigma-Aldrich, St. Louis, MO, USA). From freshly cultured cells, a conidial suspension and yeast cell suspension (10^5 spores/mL and 10^6 cells/mL, respectively) were prepared in a sterile solution of 0.9% NaCl (Sigma-Aldrich, St. Louis, MO, USA). One-hundred microliters of yeast cell suspension were evenly spread over a YPD agar plate (15 mL YPDA in a 90 mm diameter Petri dish) and incubated at 25 °C. After 24-h incubation, 10 µL of conidial suspension were spotted onto the center of a PDA plate (15 mL PDA in a 90 mm diameter Petri dish). Samples destined to proteomics investigation were obtained by spotting the conidial suspension in a PDA plate previously covered with a sterile sheet of cellophane (BioRad, Hercules, CA, USA), that allowed assimilation of nutrients and full vegetative growth. The two base plates (*i.e.*, those containing the freshly spotted conidial suspension and the 24-h old yeast culture, respectively) were hermetically sealed and incubated for seven days at 25 °C, with the fungal base plate laying at the bottom. Ochratoxin-A production was evaluated after 7 days of incubation; whereas, the radial growth of mycelium and the proteomic profile were investigated over a time span ranging from 2 to 7 days of incubation.

Biological replicates were prepared for all samples and investigations. Specifically, six biological replicates were adopted to evaluate the radial growth of the mycelium; three biological replicates were employed for the determination of the OTA production; whereas biological duplicates were subjected to protein extraction and proteome evaluation.

2.2. Administration of 2-PE to mycelial cultures

Effects of the 2-PE on the growth and metabolism of *A. carbonarius* MPVA566 were induced by spotting a fix volume (5, 10 or 15 µL) of 2-PE (Sigma-Aldrich, St. Louis, MO, USA) onto a 3 × 3-cm dish of sterile filter paper. These amounts were arbitrarily chosen based on previous empirical investigation (data not shown), enabling the simulation of a mild, medium and strong inhibition of the mycelial growth and toxin production by yeast VOCs. The 2-PE embedded paper dish was subsequently glued onto the inner surface of the Petri dish lid and hermetically sealed to prevent 2-PE vapour leak.

2.3. Ochratoxin A (OTA) extraction and HPLC analysis

Production of OTA was assessed according to the protocol by Bragulat (Bragulat et al., 2001) with minor modifications. Briefly, on the seventh day of incubation, three plugs (5 mm each) were aseptically collected along the mycelium radius. One mL of methanol was added to each sample and vigorously shaken for 1 h at room temperature. OTA extracts were filtered through a 0.2 µm filter (Millex, Millipore Co., Bedford, Mass.). Filtrates were pooled on a sample basis (*i.e.*, three radial plugs per sample). Samples were then purified in a MycoSep 229 cleanup column specific for OTA (Romer Labs, Butzbach, Germany), according to the manufacturer's instructions prior to their measurement in a reversed-phase HPLC. OTA measurements were performed in an HPLC system equipped with two LC-10ADVP pumps, system controller SCL-10 AVP and a fluorescence detector RF-10Axl (Shimadzu, Milano, Italy). OTA separation was achieved by means of a GEMINI C18 110 A column, 250 × 4.6 mm, 5 µm (Phenomenex, Castel Maggiore, Italy).

The isocratic mobile phase was composed of water/acetonitrile/acetic acid (72:27:1% w/w/w, respectively). The column temperature was set to 40 °C and the mobile phase flow was kept constant at 1.5 mL/min. Detector excitation and emission wavelengths were set to 330 and 460 nm, respectively. The system was controlled by the Class VP-5 Shimadzu software. OTA identification was confirmed by comparing the samples retention time among the retention time of the OTA pure standard (R-Biopharm, Darmstadt, Germany) which was around 6 min. OTA quantification was assessed by means of an external calibration curve drawn in the range of 0.5–100 μg/L.

2.4. Proteomic investigation: protein extraction, quantitation and in-gel digestion

Approximately 200 mg of mycelium were aseptically scraped out the cellophane layer with the use of a scalpel blade and collected in a 15 mL tube. Samples were snap-freezed in liquid nitrogen and homogenized with mortar and pestle. Homogenized samples were collected in a new 2 mL tube containing 4-volumes extraction buffer (20 mM Tris/HCl [pH 8], 2% SDS). Samples were incubated in a horizontal shaker at 60 °C, 1400 rpm for 10 min. To each sample, 1 mL Tris-HCl buffer [20 mM Tris-HCl [pH 7.5], 0.1 mg/mL $MgCl_2$, 1 mM phenylmethanesulfonyl fluoride, 1 μL/mL benzonase (Novagen, 99% 25 U/μL)] was added and cell lysis was achieved by 5 rounds of 1 min sonication bath and 1 min rest on ice. Samples were then shaken for 10 min at 1400 rpm, 37 °C, prior to being centrifuged at 10,000 × *g* for 15 min at 4 °C. Extracted proteins floating in the supernatant phase were quantified by means of the Quick Start™ Bradford protein assay (Bio-Rad, Hercules, USA) following the manufacturer's instructions. Out of the total protein extracts, an approximate amount of 50 μg was precipitated by incubation (30 min at 4 °C) with precooled Acetone. Precipitate was resuspended in 25 μL Laemmli-buffer and heated at 95 °C for 5 min, and then purified by means of separation in the first centimeters of a one-dimensional sodium dodecyl sulphate-polyacrylamide gel electrophoresis (SDS-PAGE, 4% stacking gel, 20 mA; 12% running gel, 40 mA). Trapped proteins were subjected to overnight in-gel digestion using trypsin (Promega) (Tilocca et al., 2016). Tryptic peptides are finally eluted, purified and desalted using the stage tip protocol (Rappsilber et al., 2007). Peptides were dried in a vacuum centrifuge and stored at −20 °C until LC-MS/MS measurement.

2.5. LC-MS/MS measurement

Nano-LC-ESI-MS/MS measurements were run on an EASY-nLC 1000 system (Thermo Fisher Scientific, Germany) coupled to a Q-Exactive Plus mass spectrometer (Thermo Fisher Scientific, Germany) equipped with EASY-Spray ion source (Thermo Fisher Scientific, Germany) in the Core Facility module mass spectrometry (University of Hohenheim, Stuttgart). Tryptic peptides were resuspended and directly injected onto an EASY-Spray analytical column (PepMap RSLC C18, 2 μm 100 Å 75 μm × 250 mm column, Thermo Fisher Scientific, Germany). Operating temperature was constantly kept at 40 °C. Peptides elution was performed at a flow rate of 250 nL/min over a 240 min long gradient. Column equilibration was performed by means of 10 μL 2% solvent B (0.5% acetic acid in 80% acetonitrile) in solvent A (0.5% acetic acid). Solvent B concentration was raised from 2% to 10% in 100 min, and from 10% to 22% in the next 80 min. The following 55 min increased the solvent B concentration from 22% to 45%, and the last 10 min from 45% to 95% solvent B. Elution of the polar peptides is achieved by further 15 min isocratic flow at 95% solvent B. The MS/MS instrument was operated under the control of XCalibur software (version 4.0), Thermo Fisher Scientific Inc., USA). Survey spectra (m/z = 300–1600) were detected in the Orbitrap at a resolution of 70,000 at m/z = 200. The 10 topmost abundant precursors were selected for the subsequent fragmentation in the linear ion trap. For all measurements using the Orbitrap detector, internal calibration was performed using lock-mass ions from ambient air as described in Olsen et al. (2005).

2.6. Bioinformatic data analysis

Obtained raw data were independently searched against UniProtKB database (release October 2018) relative to *Aspergillus* spp. (UniProt ID 5052, 789,108 entries), by using MaxQuant software (v.1.5.1.2). The database-dependent search was run using cysteine carbamidomethylation as fixed modification and methionine oxidation as variable modification. A maximum of two missed cleavage sites were allowed to trypsin digestion and all considered peptides had to be fully tryptic. The Label Free Quantification (LFQ) node of the software was activated and all other software settings and parameters were kept as default; including a false discovery rate < 1%, precursor mass tolerance of 4.5 ppm after mass recalibration and a fragment ion mass tolerance of 20 ppm.

Protein annotations were inferred on the basis of the protein ontology outputted from the MaxQuant searches. These, in turn, are gathered from the protein annotation of the chosen database (*i.e.* UniProt KB). LFQ abundances of the identified proteins were subjected to statistical analysis by using Primer6 v.6 statistical software (PRIMER-E, Plymouth, UK) (Bray and Curtis, 2006).

Statistical differences occurring between sample groups and between biological duplicates were calculated by means of analysis of variance with permutations (PERMANOVA). Samples scoring significative differences ($p < 0.05$) were then subjected to SIMPER analysis in order to select the only proteins responsible for the dissimilarity between pairs of groups, with a cut-off threshold of 90% (Clarke, 1993). Selected proteins were sorted into KOG and Pfam categories by using WebMGA on-line tool (Wu et al., 2011). Heat-Maps summarizing the functional profiles of the diverse sample groups in a quantitative manner were drawn using GraphPad Prism (v. 7.00).

3. Results

3.1. Exposure to both 2-phenylethanol and yeast VOCs inhibits radial mycelial growth of A. carbonarius MPVA566

Exposure to 2-PE resulted in a significant inhibition of *A. carbonarius* MPVA566 mycelial growth. Statistical analysis did not show any significant difference among biological replicates ($p > 0.05$); whereas significant differences were registered when comparing the diameter of 2-PE-exposed samples *versus* the control ones ($p < 0.01$). Specifically, 2-PE supplementation exerted a significant inhibitory effect on the mycelial growth already at the lowest dosage administered (5 μL, $p < 0.01$ after seven days of incubation). The inhibitory effect was strongly dependent on the supplemented dosage, with a higher dosage of 2-PE linked to higher and earlier growth inhibition (Table 1). Statistical analysis throughout the incubation time reveals the rapid

Table 1
Effects of 2-phenylethanol (0, 5, 10 and 15 μL) and yeast VOCs exposure on mycelial growth and ochratoxin-A (OTA) production by *Aspergillus carbonarius* MPVA566 after seven days of incubation. Mycelial growth (cm ± SD) is calculated as the mean of two orthogonal diameters measured for each of the six biological replicates. OTA production (ng/g ± SD) was measured as the mean of three biological replicates. N.D.: not detected. Values in the same column followed by different letters are significantly different (ANOVA, $p < 0.01$).

Treatment	Colony diameter (cm)	Ochratoxin A (ng/g)
Control	6.51 ± 0.09 a	1736.92 ± 71.60 a
2-PE 5 μL	6.0 0 ± 0.00 b	918.19 ± 91.13 b
2-PE 10 μL	1.48 ± 0.58 c	0.42 ± 0.22 c
2-PE 15 μL	0.90 ± 0.03 d	N.D.
VOCs	0.90 ± 0.04 e	20.63 ± 1.75 d

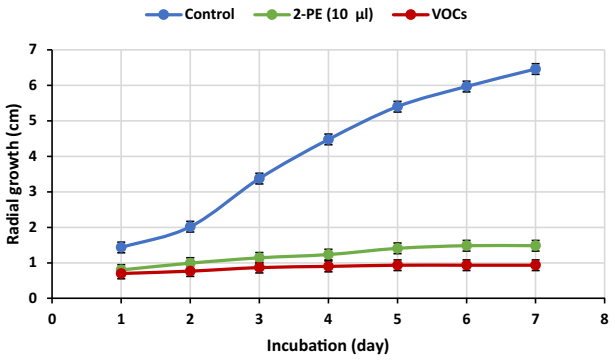

Fig. 1. Mycelial growth of *Aspergillus carbonarius* MPVA566 throughout the whole incubation period. Colony diameter (cm) of the six biological replicates for both control, VOCs and 10 µL 2-PE-exposed samples. Blue line is relative to control samples (*i.e.*, samples grown without 2-PE administration); red line is relative to the yeast VOCs-exposed samples; green line represents the fungal samples incubated in the presence of 10 µL 2-PE. Standard deviation at each timepoint is represented for both data series. (For interpretation of the references to color in this figure legend, the reader is referred to the web version of this article.)

effectiveness of the 2-PE in inhibiting mycelial growth, which was significant already after 24 h of incubation ($p < 0.01$, Fig. 1). Inhibition of the mycelial growth by VOCs released by *C. intermedia* 253 confirmed the evidence observed in the previous studies (Fig. 1; Table 1). Also, in comparison with 2-PE administration, yeast co-culture resulted in a more effective and long-lasting inhibitory effect, especially in the late incubation timepoints ($p < 0.01$).

3.2. Exposure to both 2-PE and yeast VOCs reduces OTA production by A. carbonarius MPVA566

Radial growth inhibition as induced by the 2-PE exposure was accompanied by a significant reduction of OTA production ($p < 0.01$). Table 1 show the levels of OTA in the tested samples after seven days of incubation. Here, control samples produced an average amount of 1736.93 ng/g of OTA (ranging from 1653.72 to 1828.51 ng/g). Exposure to 5 µL of 2-PE induced a reduction of the OTA level ranging from 40 to 54%, with an average production of 918.19 ng/g OTA (790.61–966.14 ng/g). Contrarywise, the administration of 10 µL 2-PE resulted in a very strong reduction of OTA production, recording an average production for the three biological replicates of 0.42 ng/g (0.23–0.74 ng/g OTA) and a relative inhibition of 99.95–99.99%. OTA production by mycelial cultures exposed to *C. intermedia* 253 VOCs is in agreement with the evidence observed in the previous reports (Farbo et al., 2018; Fiori et al., 2014): the reduction of OTA production registered in the present study achieved an average of 98.81% (Table 1).

3.3. A. carbonarius MPVA566 proteomic dataset

A total of 1882 proteins were identified across all samples; however, to increase accuracy of the obtained dataset, only the proteins identified by at least two peptides and/or one unique peptide were considered in the data analysis. Almost 1100 proteins met the chosen criteria; of these, 1025 proteins were identified in the control samples, 997 in the samples exposed to 10 µL 2-PE, and 813 proteins were identified in the mycelial samples grown in the presence of *C. intermedia* 253. A complete list of all selected proteins sorted according to the experimental treatments at the diverse incubation periods, along with its relative abundance index (LFQ) is provided as support material (S1). Relative abundance of the identified protein profile in the diverse treatment groups is depicted in Fig. 2. The great majority of identified proteins, approximately 788, was shared between all treatment groups; whereas 209 proteins were only shared between control and 2-PE supplemented

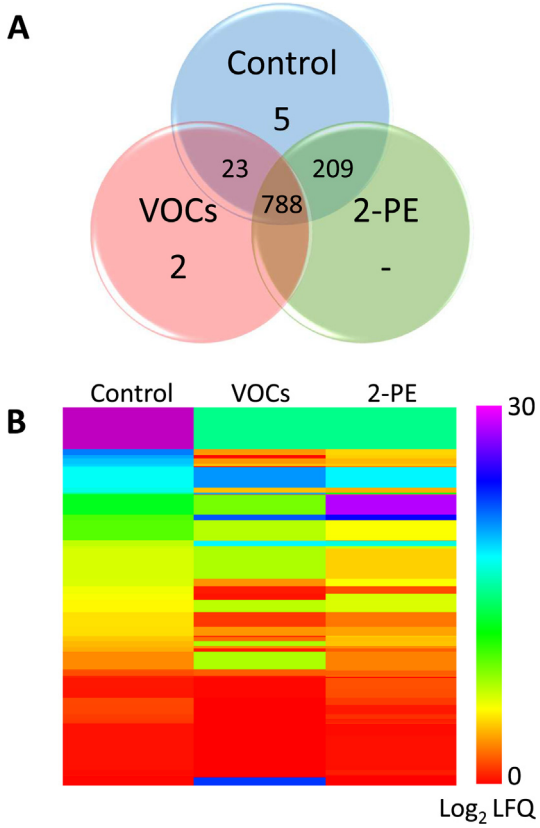

Fig. 2. Identified proteome dataset. The figure aims to provide a first introduction of the identified *Aspergillus carbonarius* MPVA566 proteomic dataset. Panel A depicts how the identified proteins are distributed along the three sample groups. The heat map in panel B displays the protein dataset and, for each of the selected proteins, provides a visual impression of its abundance level, and how it changes in the diverse growing conditions. Protein abundance is expressed as Log_2 of LFQ abundance index.

samples. Only 23 proteins were shared between the negative control and *Aspergillus* mycelium co-cultured with *C. intermedia* 253. In addition, almost no proteins were found to be uniquely expressed in each of the treatment groups; with 5 proteins identified for the sole negative control group and 2 proteins uniquely expressed in the co-cultured fungi. No uniquely expressed proteins were identified in the 2-PE supplemented samples (Fig. 2A). A heatmap highlights overall changing abundance of the identified protein list in each of the growing condition (Fig. 2B).

Analysis of variance (ANOVA) performed on the diverse treatment groups describes statistically significant differences occurring between metaproteomic datasets of the three groups of fungal samples (*i.e.* negative control, 2-PE administered and *C. intermedia* 253 co-cultured, $p = 0.01$). Also, performed ANOVA did not show any significant statistical difference among biological replicates of the experimental sample groups ($p > 0.05$).

Selected metaproteome dataset was subjected to PCoA analysis to ordinate the samples according to the experimental treatment performed (Fig. 3). Along the PCoA1, representing 34.7% of total variation, mycelial samples co-cultured with *C. intermedia* 253 are separated from other experimental groups. The latter are, instead, separated into two further clusters along the PCoA2, accounting for 22.8% of the total variation (Fig. 3). No differences were observed within the sample groups over the incubation time by means of both ANOVA and ANOVA with permutation (PERMANOVA) tests ($p > 0.05$).

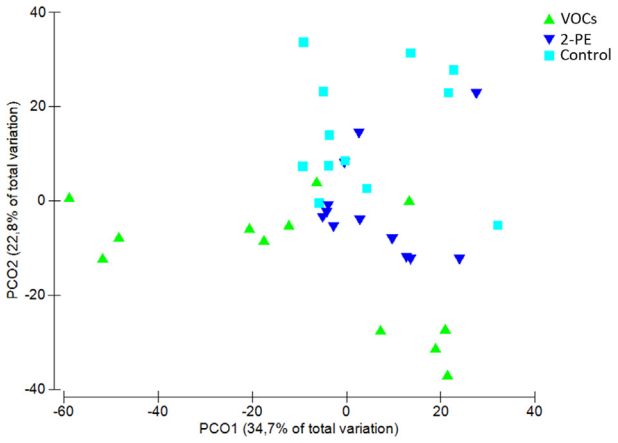

Fig. 3. Samples ordination according to PCoA analysis. Proteome dataset of the investigated samples is ordinated according to the PCoA analysis. Green triangles refer to *Aspergillus carbonarius* MPVA566 grown in the presence of VOCs arising from *Candida intermedia* 253. Blue triangles indicate the samples incubated in the presence of the sole 2-phenylethanol (2-PE); whereas the squares refer to standard culture of *A. carbonarius* MPVA566 used as a reference control. (For interpretation of the references to color in this figure legend, the reader is referred to the web version of this article.)

3.4. Metabolic shift in A. carbonarius MPVA566 as induced by C. intermedia 253 VOCs and 2-PE exposure

Proteomic datasets were subjected to SIMPER analysis to select the major protein entries responsible for the statistical dissimilarity observed between treatment groups. Selected proteins were subsequently categorised into KEGG biochemical pathways. Further functional annotation of the identified protein repertoire was achieved by the analysis of the molecular domains, motifs and functional signature, enabling the classification of the identified protein sequences into Pfam families.

The KEGG classification of the proteomic datasets is represented in Fig. 4. Here, protein pattern arising from the three diverse growing conditions are comparatively evaluated, and the only functional classes with at least two-fold abundance changes are considered. Control mycelia of *A. carbonarius* MPVA566 displayed a high abundance of KOG classes such as 60S ribosomal protein L10, 60s ribosomal protein L19, and molecular chaperones/HSP70 superfamily. Altogether, these classes support an increased concern of control samples in protein biosynthesis, maturation and delivery (Fig. 4). In both yeast co-cultured samples and 2-PE-supplemented ones, cumulative abundance of proteins belonging to "Plasma membrane H^+-transporting ATPase" accounts for as much as 2.3 times more abundant than expressed in the control samples; suggesting that both treatments exert a higher stress on the mycelial growth than the standard growing conditions (Fig. 4). Comparison of the proteomes of *A. carbonarius* MPVA566 grown in the presence of 2-PE against the yeast co-cultured ones describes the first as being more concerned in protein biosynthesis, maturation and delivery. Indeed, the abundance of "40S ribosomal protein S3", "60s ribosomal protein L19", "60S ribosomal protein L10" and "protein containing adaptin N-terminal region" KOG classes is double in the 2-PE-exposed samples compared with *C. intermedia* 253 co-cultured ones. The "40S ribosomal protein S24" KOG class, instead, is almost 11-times more abundant than yeast VOCs-exposed samples. Also, the "sphingosine phosphate lyase" KOG class is exclusively expressed in the sole 2-PE-administered samples, indicating a much higher involvement in stress response (Fig. 4). On the other hand, the samples co-cultured with *C. intermedia* 253 are uniquely expressing the "Carbon-nitrogen hydrolase" KOG class, suggesting a role of the other VOCs components (Fig. 4) in shifting the metabolic activity of *A. carbonarius* MPVA566.

Categorization of the identified protein repertoires into Pfam families confirms the high concern of the control samples in protein biosynthesis. Indeed, molecular domains attributable to ribosomal proteins were expressed as much as 10-times higher than in groups of treated samples (Fig. 5A and B). Also, functional domain of HSP-70 proteins was over 3-fold more abundantly expressed in the control samples compared to both treated samples. Heat repeats domains were also more abundant in the control samples. When control samples were compared with yeast co-cultured ones, the functional domains attributed to Heat repeats were over 10-times more abundant in control samples; whereas the abundance discrepancy was reduced to slightly > 3-fold changes in favour of the control samples when these are considered against the 2-PE-exposed samples. Similarly, the functional domains InterFeron-Related Developmental regulator (IFRD), TIP20, CLASP, and non-SMC mitotic condensation complex were more abundant in the control samples. Again, the level of abundance was over 10-times higher in the control samples when compared with yeast co-cultured samples, and slightly over 3-fold higher when compared with 2-PE-supplemented ones. Altogether, the increased levels of these functional domains are in line with the increased intracellular trafficking and proliferative activity observed in the previous KOG classification of the proteomic datasets (Figs. 4 and 5). In the pair control-*versus* yeast administered-samples, functional domains associated to flavin-binding monooxygenase, L-lysine 6 monooxygenase, and FAD-binding domain were approximately 6.5-times more abundant in the control samples; whereas the balance is around one-to-one in the pair control samples *versus* 2-PE ones. On the other hand, the samples cultured in the presence of *C. intermedia* 253 and 2-PE show a higher abundance (almost 2.5-fold) of domains related to E1–E2 ATPase, haloacid dehalogenase-like hydrolase, and cation transporter/ATPase, providing further support to the hypothesis of an increased stress condition, mirrored in the metabolic activities of *A. carbonarius* (Fig. 5A, B). In addition, the sole pair control-2-PE-sample showed increased abundance of the functional signature of AAA ATPase in 2-PE samples, suggesting the fungal cells growing under this circumstance as more involved in the extrusion of the toxic molecules (Fig. 5B).

Comparison of the protein repertoire of both treatments (*i.e.* yeast VOCs *vs* 2-PE administration) confirms the higher activity of the fungal cells exposed to 2-PE in macromolecule efflux as supported by the higher abundance of the functional domains associated to AAA ATPase (almost 7.6-fold) and HEAT repeats (2.3-fold). Domains linked to flavin-binding monooxygenase and L-lysine 6 monooxygenase are almost 8-times more represented in the 2-PE-exposed samples (Fig. 5C). Nevertheless, 2-PE samples are also featured by a higher abundance of ribosomal protein S3 and myotubularin-like phosphatase domain, suggesting a higher protein biosynthesis and transcriptional activity compared to the yeast-supplemented ones (Fig. 5C).

4. Discussion

Previous investigations demonstrated the capability of both non-fermenting (*Cyberlindnera jadinii* 273 and *Candida friedrichii* 778) and low-fermenting yeasts (*C. intermedia* 235 and *Lachancea thermotolerans* 751) in inhibiting *A. carbonarius* growth by means of VOCs production (Fiori et al., 2014). The effect of yeast-derived VOCs on *A. carbonarius* and *A. ochraceus* growth, sporulation and OTA production was further evaluated, as well as the chemical composition of the yeast-released VOCs, indicating 2-PE as the major component in all volatile cocktails (Farbo et al., 2018). The 2-PE is commonly known as the most abundant molecule responsible for the rose scent and, for this reason, it is chemically produced for cosmetic and perfumes industry (Dubois et al., 2012; Yan et al., 2011). Besides being studied for its contribution to the characteristic flavour and aroma in wine (Regodón Mateos et al., 2006), previous studies already demonstrated the antimicrobial effects of 2-PE and its ability to impact the microbial metabolism. In this view, high levels of 2-PE result in an altered protein biosynthesis along with alteration of the biochemical processes occurring at both mitochondrial

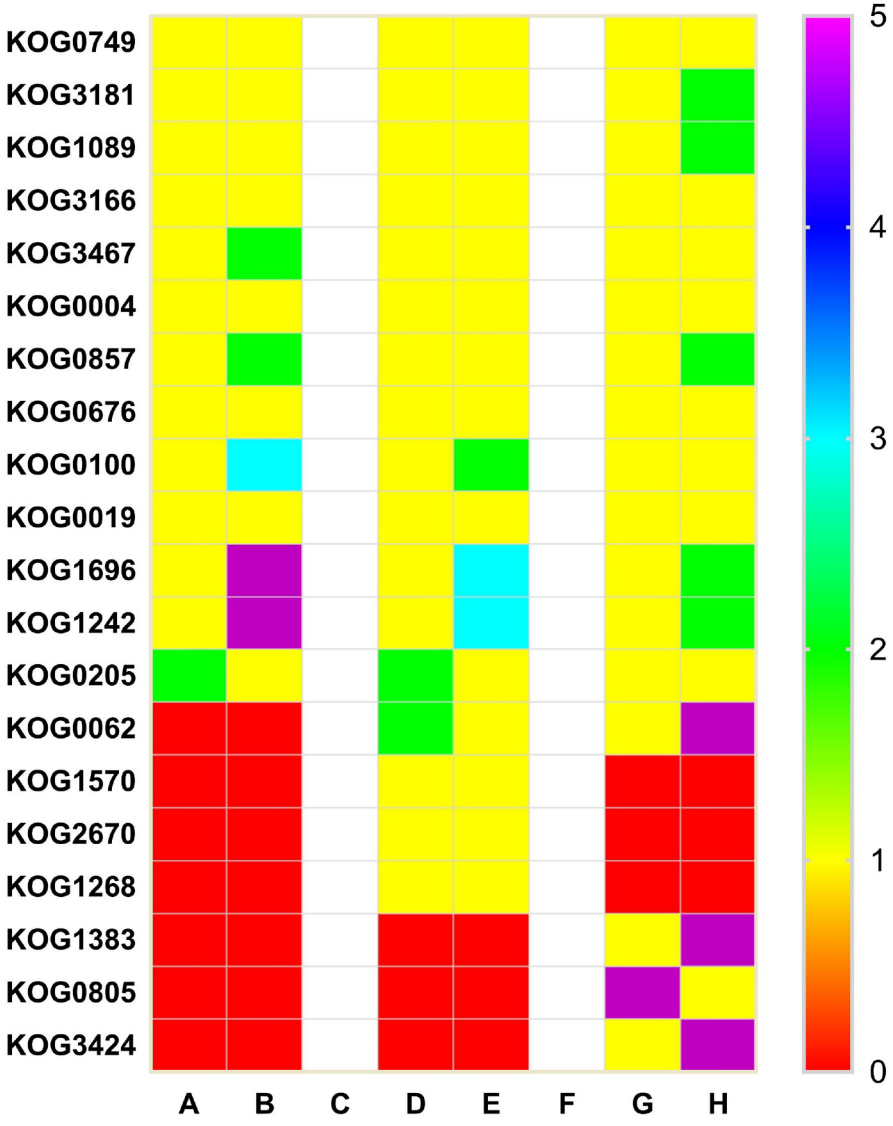

Fig. 4. Functional classification of the selected protein repertoire. The figure depicts the pairwise comparison of the KOG classes abundance identified in *Aspergillus carbonarius* MPVA566 kept at the diverse growing conditions. Abundance of the KOG classes is expressed as fold-change of the LFQ abundance index, among pair of treatments. Full names of the KOG identifiers are the following: KOG0749: Mitochondrial ADP/ATP carrier proteins; KOG3181: 40S ribosomal protein S3; KOG1089: Myotubularin-related phosphatidylinositol 3-phosphate 3-phosphatase MTM6; KOG3166: 60S ribosomal protein L7A; KOG3467: Histone H4; KOG0004: Ubiquitin/40S ribosomal protein S27a fusion; KOG0857: 60S ribosomal protein L10; KOG0676: Actin and related proteins; KOG0100: Molecular chaperones GRP78/BiP/KAR2, HSP70 superfamily; KOG0019: Molecular chaperone (HSP90 family); KOG1696: 60s ribosomal protein L19; KOG1242: Protein containing adaptin N-terminal region; KOG0205: Plasma membrane H + -transporting ATPase; KOG0062: ATPase component of ABC transporters with duplicated ATPase domains/Translation elongation factor EF-3b; KOG1570: 60S ribosomal protein L10A; KOG2670: Enolase; KOG1268: Glucosamine 6-phosphate synthetases, contain amidotransferase and phosphosugar isomerase domains; KOG1383: Glutamate decarboxylase/sphingosine phosphate lyase; KOG0805: Carbon-nitrogen hydrolase; KOG3424; 40S ribosomal protein S24.

and nuclear level (Liu et al., 2014). A possible role of 2-PE in inhibiting pathogen growth and mycotoxin production was observed by Huang et al. (2011), who reported inhibited mycelial growth of *Botrytis cinerea* by means of *C. intermedia*-derived VOCs. Accordingly, other studies described the ability of 2-PE to reduce vitality, spore germination and aflatoxin production by *A. flavus* strains (Chang et al., 2015; Huang et al., 2011). Owing to the proven effect of VOCs in inhibiting mycelial growth, this study adopted for the first time a proteomic approach to investigate the metabolic profile of an OTA-producing strain of *A. carbonarius* under three diverse growing conditions (*i.e.* exposure to 2-PE or to yeast VOCs, and standard incubation, used as a control). This enabled us to elucidate whether the previously observed effects are solely attributable to the most abundant VOCs component (*i.e.* 2-PE) or if a synergistic effect of all VOCs components is required to achieve inhibition of fungal metabolism, including OTA-production. Macroscopically, cultivation of *A. carbonarius* under exposure to 2-PE resulted in immediate and effective inhibition of the mycelial growth, even when administered in low quantity. This observation is in line with the hypothesis raised by Farbo and colleagues (Farbo et al., 2018) and is the first evidence that 2-PE reproduces the inhibitory effects observed by yeast VOCs. The low-dosage and rapid effectiveness of 2-PE administration are most likely due to the high volatility of the molecule in its pure status, resulting in a quick saturation of the growing environment and a continuous exposure of the mycelia to the inhibitory compound. Nevertheless, the low-dosage effectiveness of 2-PE was not confirmed for OTA production, since the administration of 5 µL 2-PE only influenced the vegetative growth rate but was still insufficient for an effective impact of *A. carbonarius* at a metabolic level. This hypothesis was further supported by the fact that doubling the 2-PE dosage resulted in almost complete inhibition of OTA production. Further, it suggested the minimal dosage required to investigate the metabolic effects of 2-PE administration.

The present proteomic investigation did not highlight any class of proteins as being exclusively expressed in a specific group of samples. This suggests that neither 2-PE or yeast VOCs activate further biochemical pathways than those normally contemplated. Instead, differences in the proteomics datasets from the diverse treatment groups are due to the diverse abundance levels of shared proteins.

Statistical investigation of the proteomic datasets enabled the sorting of the samples into three different groups according to the experimental treatments. This is in agreement with the previous statistical classification performed on the basis of the radial growth (Farbo et al., 2018; Fiori et al., 2014). Moreover, the lack of significant differences among the biological replicates allows indicating, with a good confidence level, the discriminative factor as the sole growing conditions *A. carbonarius* was subjected to. No statistical differences were scored while attempting to investigate the overtime dynamics of the proteome of *A. carbonarius* grown in the presence of either yeast VOCs or 2-PE.

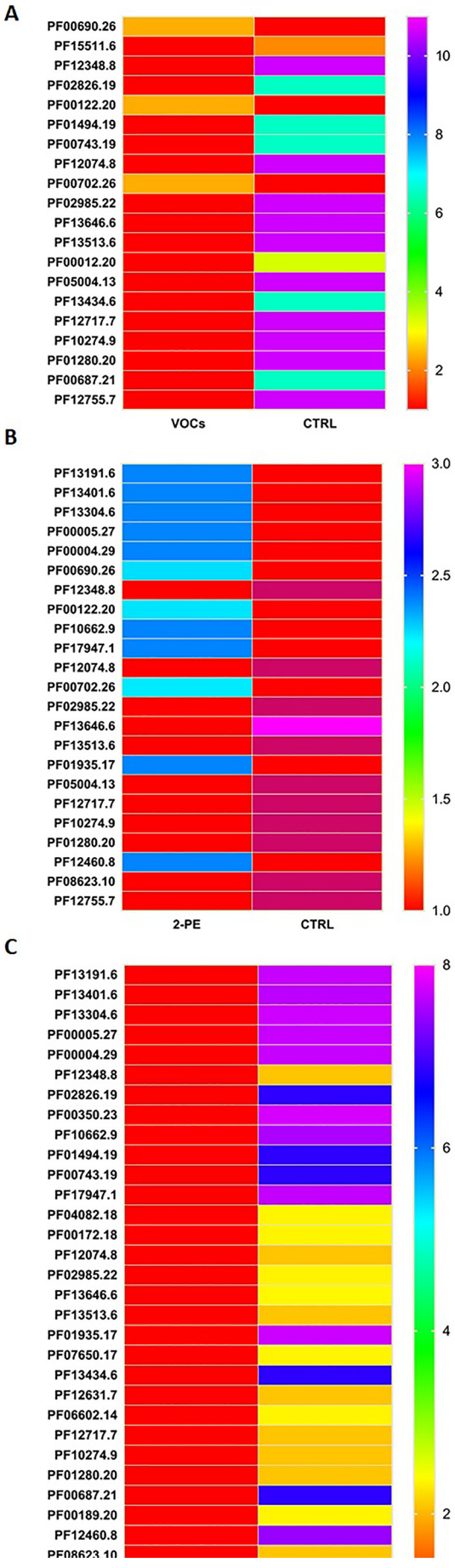

Fig. 5. Sorting of the selected proteome into Pfam database. The figure displays the cumulative abundance of the Pfam domains identified in the selected proteome of *Aspergillus carbonarius* MPVA566. Pairwise comparison of Pfam repertoires are expressed as a fold change of the cumulative LFQ indexes. Panel A compare overall abundance of the Pfam domain identified in the control samples compared to *A. carbonarius* grown in the presence of yeast VOCs. Panel B concern the pair control samples in relation to 2-phenylethanol (2-PE) administered samples. Panel C compare the yeast VOCs samples *versus* the 2-PE administered ones.
Full names of the Pfam database identifiers are listed as follow:
PF13191.6: AAA ATPase domain; PF13401.6: AAA domain; PF13304.6: AAA domain, putative AbiEii toxin, Type IV TA system; PF00005.27: ABC transporter; PF00004.29: ATPase family associated with various cellular activities (AAA); PF12348.8: CLASP N terminal; PF02826.19: D-isomer specific 2-hydroxyacid dehydrogenase, NAD binding domain; PF00350.23: Dynamin family; PF10662.9: Ethanolamine utilisation–propanediol utilisation; PF01494.19: FAD binding domain; PF00743.19: Flavin-binding monooxygenase-like; PF17947.1: Four helical bundle domain; PF04082.18: Fungal specific transcription factor domain; PF00172.18: Fungal Zn(2)-Cys(6) binuclear cluster domain; PF12074.8: General control nonderepressible 1 (Gcn1) N-terminal; PF02985.22: HEAT repeat; PF13646.6: HEAT repeats; PF13513.6: HEAT-like repeat; PF01935.17: Helicase HerA, central domain; PF07650.17: KH domain; PF13434.6: L-lysine 6-monooxygenase (NADPH-requiring); PF12631.7: MnmE helical domain; PF06602.14: Myotubularin-like phosphatase domain; PF12717.7: non-SMC mitotic condensation complex subunit 1; PF10274.9: Parkin co-regulated protein; PF01280.20: Ribosomal protein L19e; PF00687.21: Ribosomal protein L1p/L10e family; PF00189.20: Ribosomal protein S3, C-terminal domain; PF12460.8: RNAPII transcription regulator C-terminal; PF08623.10: TATA-binding protein interacting (TIP20); PF08064.13: UME (NUC010) domain; PF12755.7: Vacuolar 14 Fab1-binding region; PF00690.26: Cation transporter/ATPase, N-terminus; PF00122.20: E1-E2 ATPase; PF00702.26: haloacid dehalogenase-like hydrolase; PF05004.13: Interferon-related developmental regulator (IFRD); PF15511.6: Centromere kinetochore component CENP-T histone fold; PF00012.20: Hsp70 protein.

This might be explained by the immediate effectiveness of the VOCs and 2-PE administration on fungal metabolism. It is noteworthy that, based on the OTA production evidence, proteomic investigations were performed with high dosage (10 µL) 2-PE administration and a further comparison with the proteome upon 5 µL exposure would be useful to verify whether or not the reduced dosage of 2-PE is also affecting fungal metabolism.

Comparative evaluation of the functional profiles revealed that control samples are highly concerned in active metabolic routes such as protein biosynthesis and cell proliferation. Examples of KOG classes supporting these findings rely on the identification of diverse ribosomal proteins, along with other proteins involved in cellular trafficking. The “60S ribosomal protein L19”, for instance, has been found to be a key player of the initiation of the transcription process (Ben-Shem et al., 2011). Members of the HSP 70 superfamily have shown, in yeast model, to be involved in delivering pre-proteins for their subsequent membrane translocation (Young et al., 2003). The increased concern of control samples in protein biosynthesis is also accompanied by increased cellular trafficking, as supported by the high abundance of proteins containing adaptin N-terminal region. Role of these proteins is to select and channel the transferring direction of cargo vesicles containing the newly synthesized proteins (McMahon and Mills, 2004; Voglmaier and Edwards, 2007).

On the other hand, both VOCs- and 2-PE-exposed samples show a higher effect on stress response metabolism compared to control samples. This is supported by the increased levels of “plasma membrane H^+-transporting ATPase”, “E1-E2 ATPase”, “haloacid dehalogenase-like hydrolase”, “cation transporter/ATPase, N-terminus”. Previous studies performed in plants, linked the increased expression of these proteins to two stress events, one of which is represented by a direct effect of toxic compounds on metabolism (Gevaudant et al., 2007). On this basis, we speculate that both yeast VOCs and 2-PE administration stimulate stress response mechanisms in the fungal cells, but stress

induced to *A. carbonarius* may have a different origin for each sample group. Indeed, 2-PE samples have registered higher abundance of "sphingosine phosphate lyase" which, in yeast cells, have shown to be strongly linked to a cascade of catabolic reactions triggered as a response to heat stress (Bourquin et al., 2010; Oskouian and Saba, 2004). Whereas, mycelium samples co-cultured with *C. intermedia* 253 registered a high expression of proteins with "carbon-nitrogen hydrolase" region. This domain has been found in numerous enzymes involved in the reduction of nitrogen compounds and has also been matched against the yeast phenotype "resistance to chemicals" (Bork and Koonin, 1994; Suda et al., 2003). This is in line with our experimental treatments, suggesting that although in a tiny amount, different molecules present in the yeast volatilome may be involved in the metabolic impact and possibly in fungal inhibition. Accordingly, no expression of this domain has been identified in the 2-PE samples, as it was the only administered compound and there was no need, for the fungal cells, to reduce organic nitrogen.

The observations of our study are in accordance with a previous investigation (Fialho et al., 2016) aiming at elucidating the proteomic response of the *Citrus* pathogen *Phyllosticta citricarpa* to a mimicked VOCs mixture originally identified in *S. cerevisiae*. Although the reconstituted VOCs composition differs from the volatiles produced by *C. intermedia* 253 (Farbo et al., 2018), a similar plurality of metabolic targets was identified, with central metabolism, energy production and stress response being the most concerned routes. Nevertheless, we noticed a stronger effect of VOCs on protein biosynthesis, and intra- and inter-cellular trafficking of vesicles which can, in turn, be attributed to both protein biosynthesis and toxic compounds translocation. Moreover, we aimed at elucidating differences existing between 2-PE, the major constituent of the VOCs cocktail and the whole molecular mixture, whereas this compound was present only in traces in the *S. cerevisiae* organic volatilome.

The functional classification of the identified proteins on the basis of the Pfam domains confirmed the functional representation provided by KOG classes. Here, the protein biosynthetic activity of the control samples is further supported by the identification, in a higher abundance, of Heat repeats domains. These are commonly associated with a dense cellular trafficking (Andrade and Bork, 1995; Barford et al., 1999). Also, owing to the minor discrepancy in the Heat repeats domains abundance in the pair 2-PE/control than the pair VOCs/control, we presume that protein biosynthesis is higher in 2-PE than in VOCs ones.

In addition, Pfam domains identification emphasizes the proliferative activity of the control samples as supported by the higher abundance of dedicated molecular region such as CENP-T domain, present in a family of vertebral kinetochore proteins associated with chromatin, and are most likely involved in the structural rearrangement of the genetic material prior to cell proliferation (Nishino et al., 2012). The increased abundance of H4 histones in the control sample supports the increased proliferative activity, besides indicating the folding rearrangement of the DNA structure as a strategy to regulate its transcription (Tagami et al., 2004).

Domains associated with flavin-binding monooxygenase, L-lysine 6 monooxygenase, and FAD-binding domain are all involved in the oxidation of xeno-substrates in order to facilitate their subsequent excretion from living organisms (Cashman, 1995; Eswaramoorthy et al., 2006; Krueger and Williams, 2005; Poulsen and Ziegler, 1995). Nevertheless, in the pairwise comparison control/VOCs samples, the abundance of these proteins was higher than in the VOCs samples. Also, when VOCs samples are compared against 2-PE ones, the latter expressed these domains in a higher abundance. A plausible explanation may be that, unlike 2-PE, VOCs of yeast origin hurdle the *A. carbonarius* growth by interfering with a plurality of metabolic routes. Thus, in addition to metabolic features commonly targeted by both 2-PE and yeast VOCs, the latter also inhibit the fungal "detoxification" system, leading to a potentially longer effect than the administration of the only 2-PE may achieve. This hypothesis is also in accordance with the increased abundance of the AAA and heat repeats domains in the 2-PE-treated samples, indicating a strong energy-depending effort of these cells in translocation of the toxic compound, most likely out of the inner cellular environment (Andrade and Bork, 1995; Barford et al., 1999; Erzberger and Berger, 2006; Frickey and Lupas, 2004). Nevertheless, further long-term investigations are required to validate this hypothesis.

5. Conclusion

To the best of our knowledge, this study represents the first proteomic analysis of the impact of VOCs and 2-PE on a mycotoxigenic fungus. The interpretation of the functional data brings us to speculate that volatile compounds arising from the biocontrol yeast *C. intermedia* 253 inhibit the mycelial growth by impacting various metabolic routes of fungal system biology. Reproduction of these effects by supplementing pure 2-PE (*i.e.* the major component of the VOCs mixture) was only partially possible. Specifically, 2-PE induced macroscopic radial growth inhibition and the impact of some metabolic traits; however, other minor and still unidentified VOCs components may involve a plurality of metabolic targets, that may result in a higher effectiveness of the treatment over the long-term period. On this basis, further investigation and integration of other -omics sciences, such as metabolomics, are desirable to provide a clearer and more comprehensive picture of this biological interaction.

It has not escaped our notice that, due to its strong antifungal and mycotoxin-inhibiting activity, fumigation with pure 2-PE may be exploited as a powerful tool to preserve food and feed commodities in tightly closed environments. However, due to the multifaceted effects of 2-PE on fungal metabolism, further studies aiming to evaluate its impact on non-target biological systems are strongly encouraged.

Supplementary data to this article can be found online at https://doi.org/10.1016/j.ijfoodmicro.2019.108265.

Acknowledgements

This publication was made possible by NPRP grant # 8-392-4-003 from the Qatar National Research Fund (a member of Qatar Foundation). The findings achieved herein are solely the responsibility of the authors.

References

Adaskaveg, J.E., Förster, H., 2009. New developments in postharvest fungicide registrations for edible horticultural crops and use strategies in the United States. In: Prusky, D., Gullino, M.L. (Eds.), Post-Harvest Pathology. Springer, Dordrecht, pp. 107–117.
Andrade, M.A., Bork, P., 1995. HEAT repeats in the Huntington's disease protein. Nat. Genet. 11, 115–116.
Barford, D., Hemmings, B.A., Groves, M.R., Turowski, P., Hanlon, N., 1999. The structure of the protein phosphatase 2A PR65/A subunit reveals the conformation of its 15 tandemly repeated HEAT motifs. Cell 96, 99–110.
Ben-Shem, A., De Loubresse, N.G., Melnikov, S., Jenner, L., Yusupova, G., Yusupov, M., 2011. The structure of the eukaryotic ribosome at 3.0 Å resolution. Science 334, 1524–1529.
Bondy, G.S., Pestka, J.J., 2000. Immunomodulation by fungal toxins. J. Toxicol. Environ. Heal. - Part B Crit. Rev. 3, 109–143.
Bork, P., Koonin, E.V., 1994. A new family of carbon-nitrogen hydrolases. Protein Sci. 3, 1344–1346.
Bourquin, F., Riezman, H., Capitani, G., Grütter, M.G., 2010. Structure and function of sphingosine-1-phosphate lyase, a key enzyme of sphingolipid metabolism. Structure 18, 1054–1065.
Bragulat, M.R., Abarca, M.L., Cabañes, F.J., 2001. An easy screening method for fungi producing ochratoxin A in pure culture. Int. J. Food Microbiol. 71, 139–144.
Bray, J.R., Curtis, J.T., 2006. An ordination of the upland forest communities of southern Wisconsin. Ecol. Monogr. 27, 325–349.
Brent, K.J., Hollomon, D.W., 2007. Fungicide resistance in crop pathogens: how can it be managed? Second revised ed. FRAC, Croplife International, Brussel.
Bui-Klimke, T.R., Wu, F., 2015. Ochratoxin A and human health risk: a review of the evidence. Crit. Rev. Food Sci. Nutr. 55, 1860–1869.
Cashman, J.R., 1995. Structural and catalytic properties of the mammalian flavin-containing monooxygenase. Chem. Res. Toxicol. 8, 165–181.

Chang, P.K., Hua, S.S.T., Sarreal, S.B.L., Li, R.W., 2015. Suppression of aflatoxin biosynthesis in *Aspergillus flavus* by 2-phenylethanol is associated with stimulated growth and decreased degradation of branched-chain amino acids. Toxins 7, 3887–3902.
Clarke, K.R., 1993. Non-parametric multivariate analyses of changes in community structure. Aust. J. Ecol. 18, 117–143.
Deising, H.B., Reimann, S., Pascholati, S.F., 2008. Mechanisms and significance of fungicide resistance. Braz. J. Microbiol. 39, 286–295.
Duarte, S.C., Pena, A., Lino, C.M., 2011. Human ochratoxin A biomarkers—from exposure to effect. Crit. Rev. Toxicol. 41, 187–212.
Dubois, A., Carrere, S., Raymond, O., Pouvreau, B., Cottret, L., Roccia, A., Onesto, J.P., Sakr, S., Atanassova, R., Baudino, S., Foucher, F., Bris, M.L., Gouzy, J., Bendahmane, M., 2012. Transcriptome database resource and gene expression atlas for the rose. BMC Genomics 13, 638.
Erzberger, J.P., Berger, J.M., 2006. Evolutionary relationships and structural mechanisms of AAA+ proteins. Annu. Rev. Biophys. Biomol. Struct. 35, 93–114.
Eswaramoorthy, S., Bonanno, J.B., Burley, S.K., Swaminathan, S., 2006. Mechanism of action of a flavin-containing monooxygenase. Proc. Natl. Acad. Sci. 103, 9832–9837.
Farbo, M.G., Urgeghe, P.P., Fiori, S., Marcello, A., Oggiano, S., Balmas, V., Hassan, Z.U., Jaoua, S., Migheli, Q., 2018. Effect of yeast volatile organic compounds on ochratoxin A-producing *Aspergillus carbonarius* and *A. ochraceus*. Int. J. Food Microbiol. 284, 1–10.
Fazekas, B., Tar, A., Kovács, M., 2005. Ochratoxin A content of urine samples of healthy humans in Hungary. Acta Vet. Hung. 53, 35–44.
Fialho, M.B., de Andrade, A., Bonatto, J.M.C., Salvato, F., Labate, C.A., Pascholati, S.F., 2016. Proteomic response of the phytopathogen *Phyllosticta citricarpa* to antimicrobial volatile organic compounds from *Saccharomyces cerevisiae*. Microbiol. Res. 183, 1–7.
Fiori, S., Urgeghe, P.P., Hammami, W., Razzu, S., Jaoua, S., Migheli, Q., 2014. Biocontrol activity of four non- and low-fermenting yeast strains against *Aspergillus carbonarius* and their ability to remove ochratoxin A from grape juice. Int. J. Food Microbiol. 189, 45–50.
Frickey, T., Lupas, A.N., 2004. Phylogenetic analysis of AAA proteins. J. Struct. Biol. 146, 2–10.
Gevaudant, F., Duby, G., von Stedingk, E., Zhao, R., Morsomme, P., Boutry, M., 2007. Expression of a constitutively activated plasma membrane H^+-ATPase alters plant development and increases salt tolerance. Plant Physiol. 144, 1763–1776.
Haighton, L.A., Lynch, B.S., Magnuson, B.A., Nestmann, E.R., 2012. A reassessment of risk associated with dietary intake of ochratoxin A based on a lifetime exposure model. Crit. Rev. Toxicol. 42, 147–168.
Huang, R., Li, G.Q., Zhang, J., Yang, L., Che, H.J., Jiang, D.H., Huang, H.C., 2011. Control of postharvest botrytis fruit rot of strawberry by volatile organic compounds of *Candida intermedia*. Phytopathology 101, 859–869.
Kogkaki, E.A., Natskoulis, P.I., Magan, N., Panagou, E.Z., 2015. Effect of interaction between *Aspergillus carbonarius* and non-ochratoxigenic grape-associated fungal isolates on growth and ochratoxin A production at different water activities and temperatures. Food Microbiol. 46, 521–527.
Krueger, S.K., Williams, D.E., 2005. Mammalian flavin-containing monooxygenases: structure/function, genetic polymorphisms and role in drug metabolism. Pharmacol. Ther. 106, 357–387.
Liu, J., Wisniewski, M., Droby, S., Tian, S., Hershkovitz, V., Tworkoski, T., 2011a. Effect of heat shock treatment on stress tolerance and biocontrol efficacy of *Metschnikowia fructicola*. FEMS Microbiol. Ecol. 76, 145–155.
Liu, J., Wisniewski, M., Droby, S., Vero, S., Tian, S., Hershkovitz, V., 2011b. Glycine betaine improves oxidative stress tolerance and biocontrol efficacy of the antagonistic yeast *Cystofilobasidium infirmominiatum*. Int. J. Food Microbiol. 146, 76–83.
Liu, J., Sui, Y., Wisniewski, M., Droby, S., Liu, Y., 2013. Review: utilization of antagonistic yeasts to manage postharvest fungal diseases of fruit. Int. J. Food Microbiol. 167, 153–160.
Liu, P., Cheng, Y., Yang, M., Liu, Y., Chen, K., Long, C.A., Deng, X., 2014. Mechanisms of action for 2-phenylethanol isolated from *Kloeckera apiculata* in control of Penicillium molds of citrus fruits. BMC Microbiol. 14, 242.
Lucas, J.A., Hawkins, N.J., Fraaije, B.A., 2015. The evolution of fungicide resistance. Adv. Appl. Microbiol. 90, 29–92.
McMahon, H.T., Mills, I.G., 2004. COP and clathrin-coated vesicle budding: different pathways, common approaches. Curr. Opin. Cell Biol. 16, 379–391.
Melin, P., Håkansson, S., Schnürer, J., 2007. Optimisation and comparison of liquid and dry formulations of the biocontrol yeast *Pichia anomala* J121. Appl. Microbiol. Biotechnol. 73, 1008–1016.
Nishino, T., Takeuchi, K., Gascoigne, K.E., Suzuki, A., Hori, T., Oyama, T., Morikawa, K., Cheeseman, I.M., Fukagawa, T., 2012. CENP-T-W-S-X forms a unique centromeric chromatin structure with a histone-like fold. Cell 148, 487–501.
Nunes, C.A., 2012. Biological control of postharvest diseases of fruit. Eur. J. Plant Pathol. 133, 181–196.
Olsen, J.V., de Godoy, L.M., Li, G., Macek, B., Mortensen, P., Pesch, R., Makarov, A., Lange, O., Horning, S., Mann, M., 2005. Parts per million mass accuracy on an Orbitrap mass spectrometer via lock mass injection into a C-trap. Mol. Cell. Proteomics 4, 2010–2021.
Oskouian, B., Saba, J.D., 2004. Death and taxis: what non-mammalian models tell us about sphingosine-1-phosphate. Semin. Cell Dev. Biol. 15, 529–540.
Pfaller, M.A., Diekema, D.J., 2004. Rare and emerging opportunistic fungal pathogens: concern for resistance beyond *Candida albicans* and *Aspergillus fumigatus*. J. Clin. Microbiol. 42, 4419–4431.
Poulsen, L.L., Ziegler, D.M., 1995. Multisubstrate flavin-containing monooxygenases: applications of mechanism to specificity. Chem. Biol. Interact. 96, 57–73.
Rappsilber, J., Mann, M., Ishihama, Y., 2007. Protocol for micro-purification, enrichment, pre-fractionation and storage of peptides for proteomics using StageTips. Nat. Protoc. 2, 1896–1906.
Regodón Mateos, J.A., Pérez-Nevado, F., Ramírez Fernández, M., 2006. Influence of *Saccharomyces cerevisiae* yeast strain on the major volatile compounds of wine. Enzym. Microb. Technol. 40, 151–157.
Snelders, E., Van Der Lee, H.A.L., Kuijpers, J., Rijs, A.J.M.M., Varga, J., Samson, R.A., Mellado, E., Donders, A.R.T., Melchers, W.J.G., Verweij, P.E., 2008. Emergence of azole resistance in *Aspergillus fumigatus* and spread of a single resistance mechanism. PLoS Med. 5, e219.
Spadaro, D., Gullino, M.L., 2004. State of the art and future prospects of the biological control of postharvest fruit diseases. Int. J. Food Microbiol. 91, 185–194.
Suda, Y., Tachikawa, H., Yokota, A., Nakanishi, H., Yamashita, N., Miura, Y., Takahashi, N., 2003. *Saccharomyces cerevisiae* QNS1 codes for NAD^+ synthetase that is functionally conserved in mammals. Yeast 20, 995–1005.
Tagami, H., Ray-Gallet, D., Almouzni, G., Nakatani, Y., 2004. Histone H3.1 and H3.3 complexes mediate nucleosome assembly pathways dependent or independent of DNA synthesis. Cell 116, 51–61.
Tilocca, B., Witzig, M., Rodehutscord, M., Seifert, J., 2016. Variations of phosphorous accessibility causing changes in microbiome functions in the gastrointestinal tract of chickens. PLoS One 11, e0164735.
Tribe, H.T., Baker, K.F., Cook, R.J., 2006. Biological control of plant pathogens. J. Appl. Ecol. 12, 983.
Voglmaier, S.M., Edwards, R.H., 2007. Do different endocytic pathways make different synaptic vesicles? Curr. Opin. Neurobiol. 17, 374–380.
Wu, S., Zhu, Z., Fu, L., Niu, B., Li, W., 2011. WebMGA: a customizable web server for fast metagenomic sequence analysis. BMC Genomics 12, 444.
Yan, H., Zhang, H., Wang, Q., Jian, H., Qiu, X., Wang, J., Tang, K., 2011. Isolation and identification of a putative scent-related gene RhMYB1 from rose. Mol. Biol. Rep. 38, 4475–4482.
Young, J.C., Hoogenraad, N.J., Hartl, F.U., 2003. Molecular chaperones Hsp90 and Hsp70 deliver preproteins to the mitochondrial import receptor Tom70. Cell 112, 41–50.